

# Thermal shock resistance and fracture toughness of liquid-phase-sintered SiC-based ceramics

Alexandra Kovalčíková<sup>a,\*</sup>, Ján Dusza<sup>a</sup>, Pavol Šajgalík<sup>b</sup>

<sup>a</sup> Institute of Materials Research, Slovak Academy of Sciences, Watsonova 47, 040 01 Košice, Slovak Republic

<sup>b</sup> Institute of Inorganic Chemistry, Slovak Academy of Sciences, Dúbravská cesta 9, 845 36 Bratislava 45, Slovak Republic

Received 30 September 2008; received in revised form 12 January 2009; accepted 19 January 2009

Available online 23 February 2009

## Abstract

The effect of the heat treatment on the toughness and thermal shock resistance of the silicon carbide–silicon nitride composites prepared by liquid-phase-sintering was investigated. The fracture toughness has been estimated using the indentation method and the thermal shock resistance was studied using the indentation-quench method. The results were compared to those obtained for a reference silicon carbide material, prepared by the same fabrication route. The indentation toughness increased from 2.88 to 5.39 MPa m<sup>1/2</sup> due to the toughening mechanisms (crack deflection, mechanical interlocking and crack branching) occurring in the heat-treated materials during the crack propagation. Similarly the thermal shock resistance increased after the heat treatment of the experimental materials.

© 2009 Elsevier Ltd. All rights reserved.

**Keywords:** SiC; Composites; Heat treatment; Toughness and toughening; Thermal shock resistance

## 1. Introduction

Silicon carbide and silicon nitride have been recognised as important structural ceramics because of their good combination of mechanical and thermal properties. SiC ceramics show good wear, creep and oxidation resistance at high temperatures, but relatively low fracture toughness. On the contrary, Si<sub>3</sub>N<sub>4</sub> ceramics exhibit higher fracture toughness and good flexural strength, but lower resistance to oxidation at high temperatures.<sup>1</sup> Silicon carbide is a promising material for high temperature applications (heat engines, heat exchangers, and many other devices), however it is difficult to densify without sintering additives because of the covalent nature of Si–C bonding and low self-diffusion coefficient. Components to be properly applied in high temperature need to have a high resistance to thermal shock, thermal fatigue, corrosion, and resistance to creep deformation. Si-based ceramics such as silicon carbide and silicon nitride due to their covalent bonding exhibit a high strength at elevated temperature (up to 1000 °C), as well as low thermal expansion coefficient and high thermal conductivity, and therefore a high resistance

to thermal shock.<sup>2–4</sup> Because of the lower fracture toughness of silicon carbide ceramics, the possibility of an in situ toughening has been investigated by many authors.<sup>5–9</sup> Toughening is obtained through the development of large elongated or platelet-shape grains that has been related to the β → α SiC transition occurring at 1800–2000 °C. Elongated grains have been shown to increase fracture toughness by crack bridging or crack deflection due to weak interface boundaries, but coarsening leads to an increase of the size of the critical flaw which degrades flexural strength.<sup>6,9–13</sup> The Vickers indentation fracture toughness test has been applied for estimation of the fracture resistance of brittle ceramics for the past three decades.<sup>14–19</sup> The techniques rapidly achieved popularity because their simplicity (only small volume of material, short preparation of samples and low financial costs). However, Quinn and Bradt<sup>20</sup> concluded that the Vickers indentation fracture toughness test is fundamentally different than the standard fracture toughness technique. This technique is not reliable as fracture toughness test for ceramics or for other brittle materials, because the crack initiation and propagation is not the same as the sequence of crack processes in the standardized fracture toughness tests. They also recommended that these tests should not be used for fracture toughness testing of ceramics, even if just for a comparative basis. The ceramic scientific community agrees with the opinion

\* Corresponding author. Tel.: +421 55 792 2463; fax: +421 55 792 2408.  
E-mail address: [avysocka@imr.saske.sk](mailto:avysocka@imr.saske.sk) (A. Kovalčíková).

of Quinn and Bradt<sup>20</sup> with regards to the fracture toughness values mainly for the unsuitability of the indentation lifetime and probability prediction of ceramic samples/parts. On the other hand it could be imagined that the measured “indentation toughness” using indentation method can offer some basic information with regards to the toughness of newly development ceramics. Also the cracks created by Vickers indenter could be useful for the study of the possible toughening mechanisms occurring also during the crack propagation under the applied load required for determination of  $K_{IC}$ .

During thermal shock, transient thermal stresses build up in the material which can become large enough to induce damage, such as microcracking or macrocracking.<sup>21</sup> The thermal shock properties of a material depend on the number of parameters such as tensile strength, fracture toughness, Young’s modulus and thermal expansion coefficients. In addition to these materials properties, which can be tabulated, the microstructure character is also of importance and influences the thermal shock behaviour of the material.<sup>22</sup> The investigation of the behaviour of Vickers indentation cracks under quenching condition has raised interest during the last years. An indentation-quench method has been developed by Andersson and Rowcliffe.<sup>23</sup> Compared to the Haselman quench-strength method,<sup>24</sup> the evaluation procedure is simple, the sample preparation is easy and only a small number of samples are needed for a series of measurements at different temperatures. The indentation-quench method can be used for the characterization of materials and as a diagnostic tool to predict the thermal shock damage occurrence in a component.<sup>25</sup> To evaluate the thermal stress crack initiation and propagation behaviour of ceramics, two thermal shock resistance parameters are usually used.<sup>26</sup> First is the resistance to initiation of crack, expressed by parameter  $R$ :

$$R = \frac{\sigma_c(1 - \nu)}{\alpha E} = \Delta T_c \quad (1)$$

where  $\sigma$  is the tensile strength,  $E$  the Young’s modulus,  $\alpha$  the coefficient of thermal expansion and  $\nu$  is the Poisson’s ratio.

Higher  $R$  represents a greater resistance to the initiation of fracture during rapid quenching and during steady-state heat flow down a steep temperature gradient. The second is the resistance to propagation of crack expressed by the parameter  $R''''$ :

$$R'''' = \left( \frac{K_{IC}}{\sigma_r} \right)^2 (1 + \nu) \quad (2)$$

which dedicates the resistance to catastrophic crack propagation of ceramics under a critical temperature difference,  $dT_c$ .

From the above two equations, it is clearly visible that the thermal shock resistance can be improved by the increased flexural strength and fracture toughness and by decreased Young’s modulus and coefficient of thermal expansion. Simultaneous increase of strength and toughness in ceramics is not always possible.<sup>2</sup> Usually ceramics with higher strength are more brittle and materials with more stable crack propagation exhibit a lower strength.

The thermal shock resistance of SiC + Si<sub>3</sub>N<sub>4</sub> composites has not yet been reported. Takeda and Maeda<sup>27</sup> showed that the

thermal shock resistance of hot pressed SiC with BeO and AlN depends on the thermal conductivity. At 100 W m<sup>-1</sup> K<sup>-1</sup>,  $\Delta T_c = 680^\circ\text{C}$  and at 65 W m<sup>-1</sup> K<sup>-1</sup>,  $\Delta T_c = 450^\circ\text{C}$ . Wang and Singh<sup>28</sup> measured for HP SiC  $\Delta T_c = 500^\circ\text{C}$  at thermal conductivity of 87 W m<sup>-1</sup> K<sup>-1</sup>. Pettersson et al.<sup>22</sup> studied the best parameters for measuring the thermal shock resistance of Si<sub>3</sub>N<sub>4</sub>-based materials with an indentation-quench method. The best resolution was obtained with a sample diameter 12 mm, height 4 mm, initial crack length 100  $\mu\text{m}$  and water temperature 90  $^\circ\text{C}$ . Many others authors have studied thermal shock resistance of different ceramics materials by water quenching or indentation tests (sintered alumina/silicon carbide nanocomposites,<sup>29</sup> alumina/zirconia functionally graded material,<sup>30</sup> Al<sub>2</sub>O<sub>3</sub>-TiC composites,<sup>31</sup> SiC-BN composites,<sup>32</sup> porous silicon carbide<sup>33</sup>).

The aim of this work is to investigate the influence of the heat treatment on the microstructure, indentation toughness and indentation thermal shock resistance of SiC and SiC + Si<sub>3</sub>N<sub>4</sub> composites.

## 2. Experimental procedure

$\beta$ -SiC powder (HSC-059, Superior Graphite) was mixed with Al<sub>2</sub>O<sub>3</sub> (A 16 SG, Alcoa), Y<sub>2</sub>O<sub>3</sub> (grade C, H.C. Starck) and Si<sub>3</sub>N<sub>4</sub> (AIY-3/54, Grade C, Plasma & Ceramic Technologies Ltd.). The Si<sub>3</sub>N<sub>4</sub> powder contains Y<sub>2</sub>O<sub>3</sub> and Al<sub>2</sub>O<sub>3</sub> sintering additives in weight ratio 6:3. The weight ratio of nonoxide matrix to oxide sintering additives SiC (+Si<sub>3</sub>N<sub>4</sub>): Y<sub>2</sub>O<sub>3</sub> + Al<sub>2</sub>O<sub>3</sub> was kept constant, 91:9. The weight ratio of particular oxides Y<sub>2</sub>O<sub>3</sub>:Al<sub>2</sub>O<sub>3</sub> was 6:3 for all compositions. The final chemical compositions of the investigated materials are listed in Table 1.

The powder mixtures were ball milled in isopropanol with SiC balls for 24 h. The suspension was dried and subsequently sieved through 25  $\mu\text{m}$  sieve screen in order to avoid hard agglomerates. The samples were sintered by hot pressing at 1850  $^\circ\text{C}/1$  h under mechanical pressure of 30 MPa in N<sub>2</sub> atmosphere. The hot pressed samples were subsequently annealed under various temperature conditions given in Table 1. After sintering and annealing the specimens were cut, polished to a 1  $\mu\text{m}$  finish and plasma etched. The microstructures were then studied using an SEM (JEOL JSM-7000F).

The densities of the sintered and annealed specimens were measured according to Archimedes’ principle. Mechanical properties were investigated using indentation methods. Hardness was determined by Vickers indentation (hardness testers LECO 700AT) under a load of 49.05 N with a dwell time of 10 s. In order to determine the indentation toughness at least 15 Vickers indentations per specimen were introduced with the load of 49.05 N. The indentation toughness was calculated from the lengths of radial cracks and indents diagonals using a formula valid for semi-circular crack systems as proposed by Anstis et al.<sup>14</sup>:

$$K_{IC} = 0.016 \left( \frac{E}{H} \right)^{1/2} \left( \frac{P}{c^{3/2}} \right) \quad (3)$$

where  $K_{IC}$ , indentation toughness (MPa m<sup>1/2</sup>); 0.016, material-independent constant for Vickers-produced radial cracks;  $E$ ,

Table 1  
Chemical composition and heat treatment regimes of the investigated materials.

Samples	Heat treatment	Composition (wt%)			
		SiC	Si <sub>3</sub> N <sub>4</sub>	Y <sub>2</sub> O <sub>3</sub>	Al <sub>2</sub> O <sub>3</sub>
SC-N0-HP	HP (1850 °C/1 h)	91	0	6	3
SC-N5-HP	HP (1850 °C/1 h)	86.5	5	5.7	2.8
SC-N10-HP	HP (1850 °C/1 h)	81.9	10	5.4	2.7
SC-N0-1650	HP (1850 °C/1 h) + AN (1650 °C/5 h)	91	0	6	3
SC-N5-1650	HP (1850 °C/1 h) + AN (1650 °C/5 h)	86.5	5	5.7	2.8
SC-N10-1650	HP (1850 °C/1 h) + AN (1650 °C/5 h)	81.9	10	5.4	2.7
SC-N0-1850	HP (1850 °C/1 h) + AN (1850 °C/5 h)	91	0	6	3
SC-N5-1850	HP (1850 °C/1 h) + AN (1850 °C/5 h)	86.5	5	5.7	2.8
SC-N10-1850	HP (1850 °C/1 h) + AN (1850 °C/5 h)	81.9	10	5.4	2.7

Young modulus (GPa);  $H$ , Vickers hardness (GPa);  $P$ , indentation load (N);  $c$ , half-length of the radial crack (m).

The flexural strength was measured using specimens with dimensions 3 mm × 4 mm × 45 mm. They were ground and polished by 15 μm diamond grinding wheel before testing. The two edges on the tensile surface were rounded with a radius about 0.15 mm in order to eliminate a failure initiated from an edge of the specimen. The specimens were tested in four point bending fixture (inner span of 20 mm and an outer span of 40 mm) with the crosshead speed of 0.5 mm/min at ambient temperature and atmosphere.

For the investigation of thermal shock resistance the indentation-quench method was used. All indentations were made with a 49.05 N load to obtain the per-cracks approximately in the same length. Pettersson et al.<sup>22</sup> in his study mentioned that the material with better thermal shock resistance can absorb the residual stress at the higher loads better than the poorer material. When too high a load is used (the initial cracks are too long) the crack growth depends both on the relaxation of residual stress in the material and on the thermal shock. A good choice seems to be an initial crack length of 100 ± 10 μm for testing of Si<sub>3</sub>N<sub>4</sub>-based ceramics. The length of the cracks was measured using optical microscopy. After the indentation the samples were heated in a vertical tube furnace in air to the required temperature and held there for 25 min. Then the specimens were rapidly immersed into a ~20 °C water bath. Final radial crack lengths were then measured with optical microscope. The procedure was repeated at increasing quenching temperatures  $\Delta T$ , up to the critical value of  $\Delta T_c$  at which radial crack became unstable and the specimen failed.

### 3. Results and discussion

Representative SEM micrographs of a polished and plasma etched surface of the monolithic SiC and SiC + Si<sub>3</sub>N<sub>4</sub> composites are shown in Fig. 1. The microstructures of hot pressed SC-N0-HP (Fig. 1a) and SC-N0-1650 material annealed at 1650 °C consist of fine submicron-sized equiaxed SiC grains with a low aspect ratio (approximately 1). No visible effect of the heat-treatment at 1650 °C was found on the microstructure of the material. In the case of SiC + Si<sub>3</sub>N<sub>4</sub> composite the addition of silicon nitride resulted in a finer microstructure of the composites (Fig. 1b and c). All the materials additionally

contain an intergranular phase in the form of a very thin grain boundary films and in the form of triple points with a size up to approximately 0.5 μm. The microstructures of the SiC material and SiC + Si<sub>3</sub>N<sub>4</sub> composites significantly changed after their post-sintering high temperature treatment at 1850 °C (Fig. 1d–f). They have a bimodal distribution and consist of elongated SiC grains with higher aspect ratio (4.4) and of smaller SiC grains.

All ceramic samples were well densified. All the specimens with oxide additives have a value of relative density above 97.2% and the addition of silicon nitride increases the density. The density was decreased by increasing the annealing temperature. The results of the hardness and indentation toughness measurements are shown in Table 2.

During heat treatment, the average grain size ( $G$ ) increased in all systems and hence invoking Hall-Petch like  $H$  vs.  $G^{1/2}$  behaviour, hence one would expect a decrease in hardness ( $H$ ) values with increasing average grain size.<sup>34</sup> However, in poly-crystalline ceramics containing glassy grain boundary and intergranular phases, after thermal treatment, reduction and crystallisation of the secondary phases generally improve the hardness of the material.<sup>10</sup> In our case no significant change in the values of hardness due to the heat treatment and silicon nitride addition has been observed.

According to the results, the indentation toughness is increased with annealing temperature. For fine-grained globular microstructure of hot pressed SiC and SiC + Si<sub>3</sub>N<sub>4</sub> composites the indentation toughness had a value of  $K_{IC,ind}$  in interval from 2.88 ± 0.2 to 2.90 ± 0.2 MPa m<sup>1/2</sup>. After heat treatment at 1650 °C the indentation toughness increased and its values changed from 3.33 ± 0.1 to 3.38 ± 0.1 MPa m<sup>1/2</sup>. For annealed materials at 1850 °C/5 h with platelet microstructure the highest indentation toughness was obtained (from 4.38 ± 0.4 to 5.39 ± 0.3 MPa m<sup>1/2</sup>). Microfractographic observations of the fracture surface and fracture profiles have shown that the crack propagation was controlled by mixed inter- and transgranular fracture in all materials with slightly higher transgranular portion in the system annealed at 1850 °C/h. In materials with fine microstructure and globular shaped grains the crack propagates mainly intergranularly with relatively small deflection from the main crack direction (Fig. 2a). At such a crack propagation there is a low probability that toughening mechanisms occur in the form of crack bridging or frictional and mechanical interlocking of the separated fracture surfaces. In the investigated

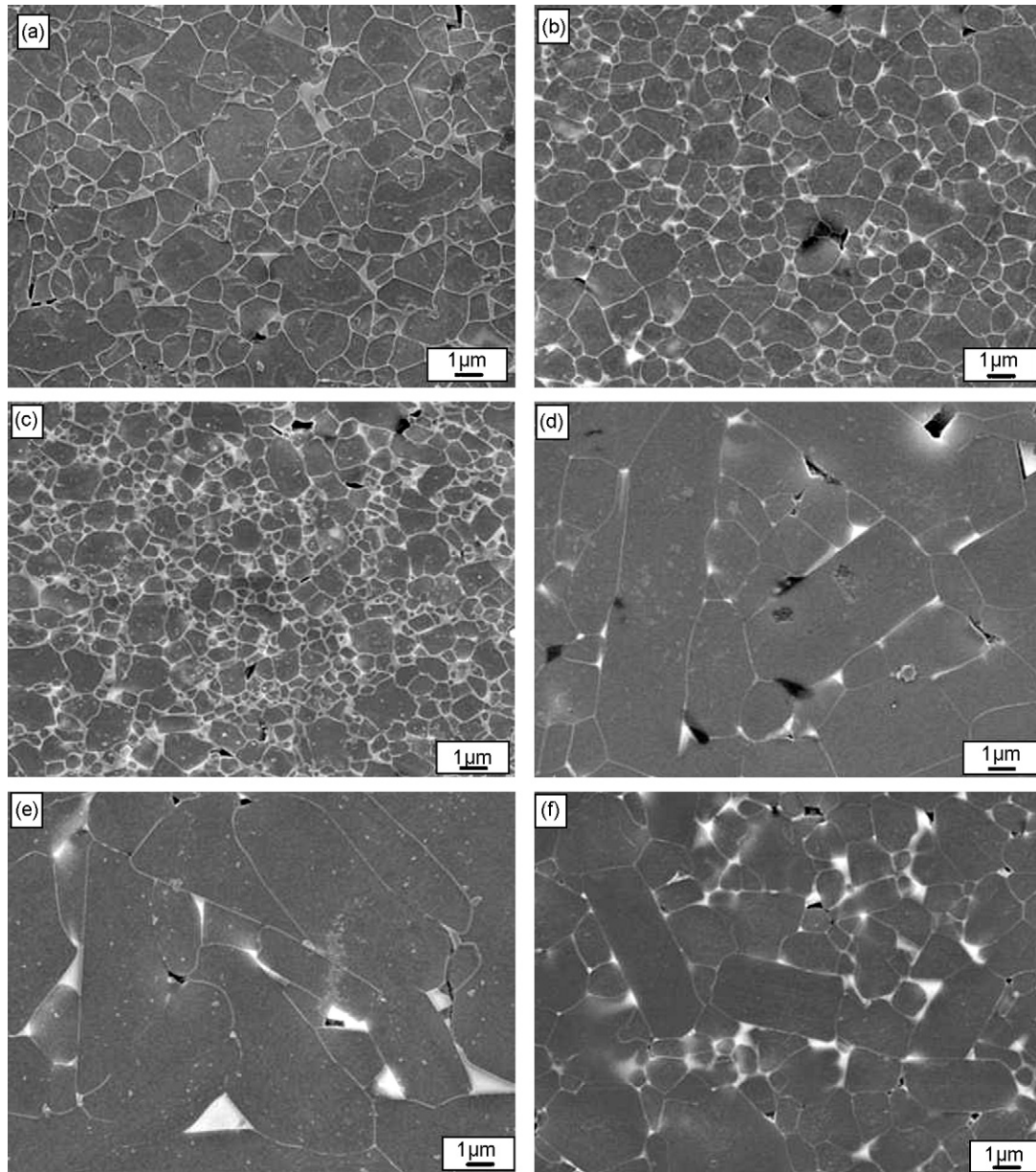


Fig. 1. SEM micrographs of (a) SC-N0-HP; (b) SC-N5-HP; (c) SC-N10-HP; (d) SC-N0-1850; (e) SC-N5-1850; (f) SC-N10-1850.

Table 2  
Properties of SiC and SiC + Si<sub>3</sub>N<sub>4</sub> composites.

Samples	Density (g/cm <sup>3</sup> )	HV5 (GPa)	$K_{IC,ind}$ (MPa m <sup>1/2</sup> )	$\sigma_{4BT}$ (MPa)	$R_{theoretic}$ (°C)	$R_{exp}$ (°C)	$R_{Tancret}$ (°C)
SC-N0-HP	3.220	20.4 ± 0.9	2.90 ± 0.2	387	228	320	340
SC-N5-HP	3.236	19.7 ± 0.6	2.88 ± 0.2	507	333	350	360
SC-N10-HP	3.249	20.6 ± 0.7	2.89 ± 0.1	584	359	500	540
SC-N0-1650	3.220	19.4 ± 1.3	3.35 ± 0.2	424	215	530	540
SC-N5-1650	3.224	20.4 ± 0.7	3.33 ± 0.1	614	346	580	590
SC-N10-1650	3.241	20.8 ± 1.1	3.38 ± 0.1	478	364	750	720
SC-N0-1850	3.189	20.6 ± 0.3	4.54 ± 0.4	142	90	650	380
SC-N5-1850	3.196	22.5 ± 0.8	5.39 ± 0.3	391	206	850	430
SC-N10-1850	3.204	20.7 ± 1.1	4.38 ± 0.4	230	136	760	400

Vickers hardness and indentation toughness were measured at the applied load of 49.05 N,  $R_{theoretic}$  was calculated from Eq. (1),  $R_{Tancret}$  was calculated by Tancret model – Ref. [31].

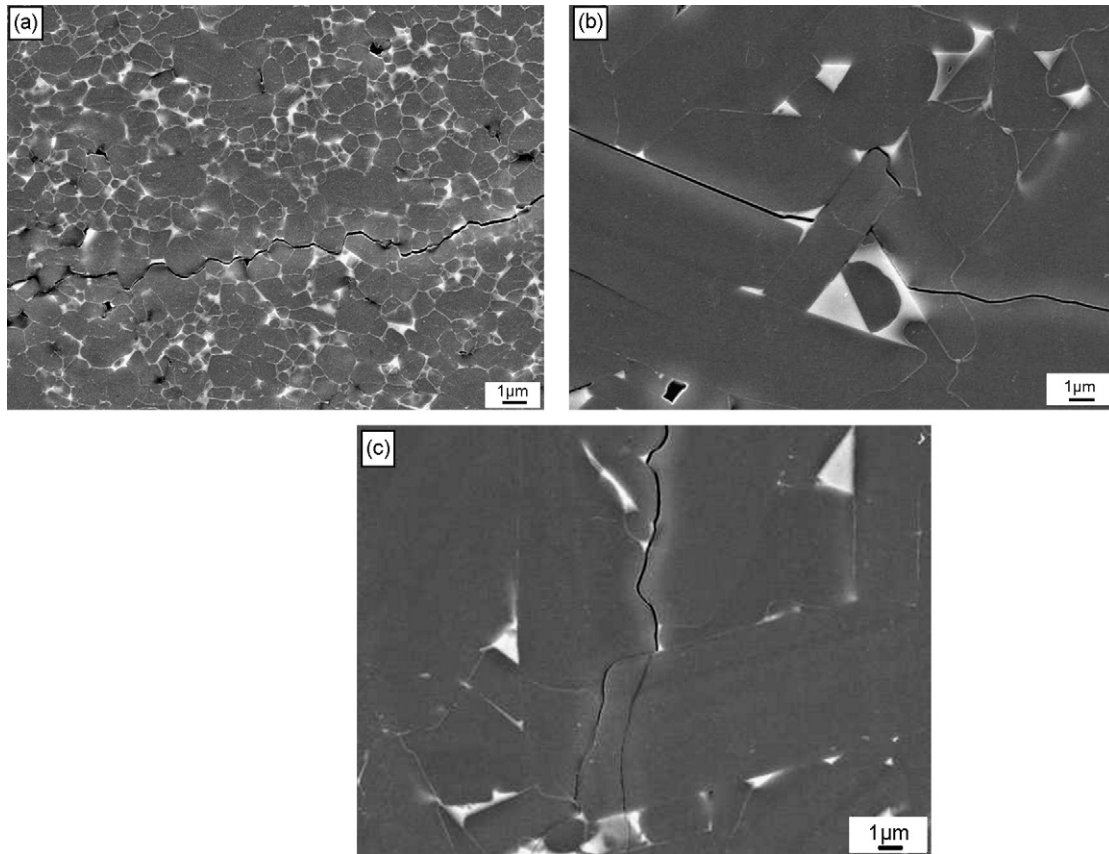


Fig. 2. Crack path after annealing: (a) SC-N0-1650; (b) SC-N0-1850, bridging; (c) SC-N5-1850, branching.

materials with coarse grains and plate-like microstructure the crack propagation is significantly different. In these materials the crack deflection is more enhanced (often up to approximately  $10\ \mu\text{m}$  from the main crack direction) (Fig. 2b) which is important itself, but also from the point of view of creation new toughening mechanisms in the bridging zone of the propagating crack. Such mechanisms have been observed in the form of frictional and mechanical interlocking of the SiC grains, usually in a relatively large distance behind the crack front. As an additional toughening mechanism crack branching has been identified very often in these systems (Fig. 2c). Such toughening mechanisms are probably responsible for the higher indentation toughness. This is in agreement with the results of similar investigations.<sup>6,7,10,35</sup> This relatively significant improvement of  $K_{IC,ind}$  upon annealing at  $1850\ ^\circ\text{C}/5\ \text{h}$  can be directly correlated with the larger grain size and higher aspect ratio despite some indication of transcrystalline fracture behaviour.

Fig. 3a shows the results of the thermal shock tests for hot pressed materials. The initial cracks size were  $\approx 120\ \mu\text{m}$  for indentation load 50 N. A critical temperatures  $\Delta T_c$  when the specimens failed are  $\sim 320\ ^\circ\text{C}$  for monolithic SiC,  $350\ ^\circ\text{C}$  for SiC composite with 5 wt%  $\text{Si}_3\text{N}_4$  and  $500\ ^\circ\text{C}$  for SiC +  $\text{Si}_3\text{N}_4$  with 10 wt% silicon nitride.

The dependence of radial crack growth on temperature for heat-treated materials at  $1650\ ^\circ\text{C}/5\ \text{h}$  is plotted in Fig. 3b. The initial cracks size were  $\approx 120\ \mu\text{m}$  for indentation load 50 N, too. From Fig. 3b are visible three different areas which char-

acterize the crack evolution after quenching: (a) an initial radial cracks growing slightly with increasing  $\Delta T$  (area to  $\Delta T \sim 200\ ^\circ\text{C}$  for SC-N0-1650, SC-N10-1650 and  $\Delta T \sim 300\ ^\circ\text{C}$  for SC-N5-1650); (b) a radial crack growing stable extension (area from  $\Delta T \sim 200\ ^\circ\text{C}$  to  $\Delta T \sim 500\ ^\circ\text{C}$  for SC-N0-1650, from  $\Delta T \sim 300\ ^\circ\text{C}$  to  $\Delta T \sim 500\ ^\circ\text{C}$  for SC-N5-1650 and from  $\Delta T \sim 200\ ^\circ\text{C}$  to  $\Delta T \sim 700\ ^\circ\text{C}$  for SC-N10-1650); (c) a radial crack growing unstable extension and the specimens failed. A critical temperatures  $\Delta T_c$  when the monolithic SiC s failed is  $\sim 530\ ^\circ\text{C}$ , above  $580\ ^\circ\text{C}$  for composite SC-N5-1650 and the highest  $\Delta T_c = 750\ ^\circ\text{C}$  was observed for composite SC-N10-1650. The propagation of Vickers indentation crack of SC-N10-1650 before thermal shock is shown in Fig. 4a, after thermal shock at  $\Delta T = 400\ ^\circ\text{C}$  in Fig. 4b and after thermal shock at  $\Delta T = 750\ ^\circ\text{C}$  in Fig. 4c.

In the case of heat-treated specimens at  $1850\ ^\circ\text{C}/5\ \text{h}$  the initial crack length was above  $100\ \mu\text{m}$  at indentation load 50 N. In Fig. 3c are visible three different areas which characterize the crack evolution after quenching: (a) an initial radial cracks growing slightly with increasing  $\Delta T$  (area to  $\Delta T \sim 200\ ^\circ\text{C}$  for all tested materials); (b) a radial crack growing stable extension (area from  $\Delta T \sim 200\ ^\circ\text{C}$  to  $\Delta T \sim 600\ ^\circ\text{C}$  for SC-N0-1850, from  $\Delta T \sim 200\ ^\circ\text{C}$  to  $\Delta T \sim 800\ ^\circ\text{C}$  for SC-N5-1850 and from  $\Delta T \sim 200\ ^\circ\text{C}$  to  $\Delta T \sim 700\ ^\circ\text{C}$  for SC-N10-1850); (c) a radial crack growing unstable extension and the specimens failed ( $\Delta T_c \sim 650\ ^\circ\text{C}$  for SC-N0-1850,  $\Delta T_c \sim 850\ ^\circ\text{C}$  for SC-N5-1850 and  $\Delta T_c \sim 760\ ^\circ\text{C}$  for SC-N10-1850). Microfrac-

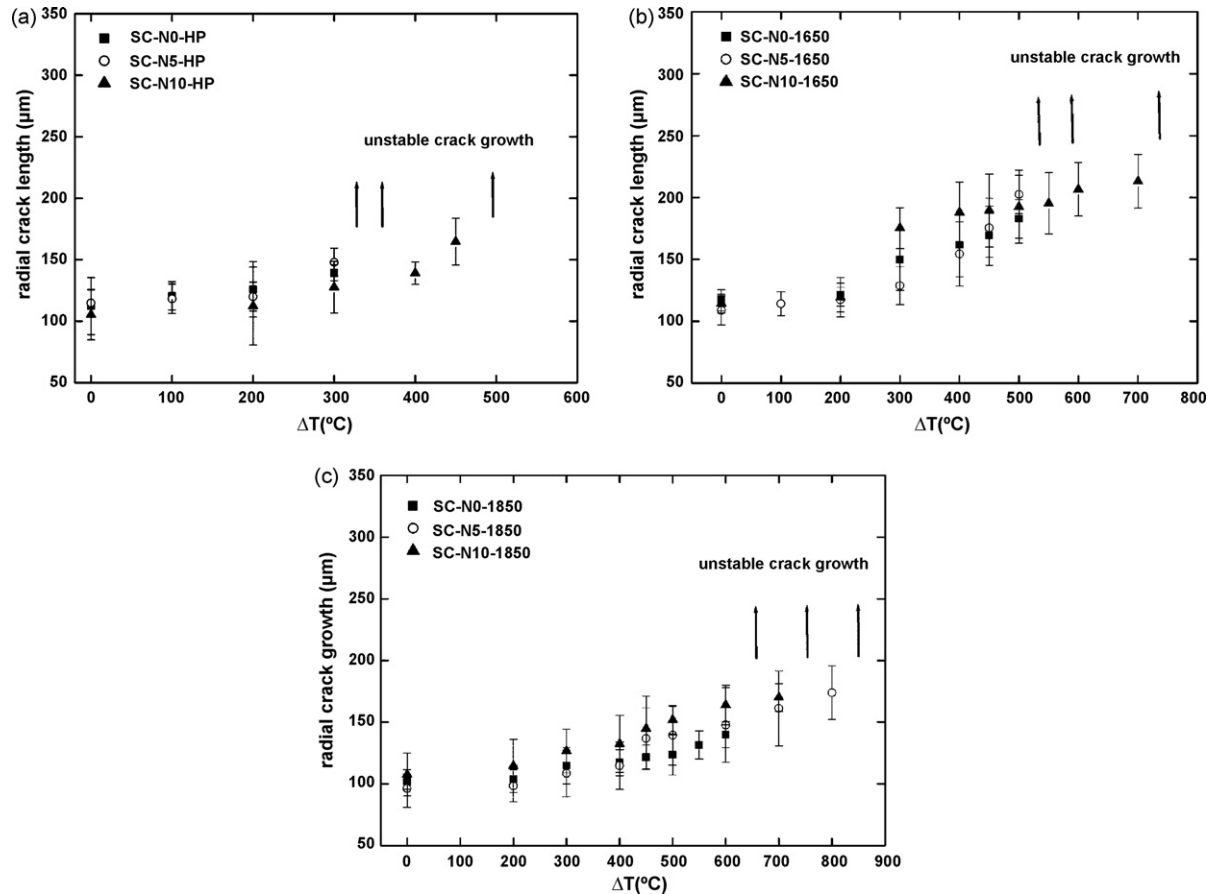


Fig. 3. Crack propagation at thermal shock tests: (a) hot-pressed materials; (b) materials annealed at 1650 °C/5 h; (c) materials annealed at 1850 °C/5 h. The temperature difference at which unstable cracking begins are marked by arrows.

tographic observation of thermally shocked specimens with Vickers indentation showed well-defined radial crack pattern. These cracks increased in size with increasing temperature, but always reached instability first in the longitudinal direction (i.e. crack aligned parallel to the specimen length). This indicates a slightly higher tension in the transverse direction, consistent with some edge effect in the thermal transfer process (via  $r_0$  in the Biot coefficient).<sup>36</sup>

For all tested specimens the rise in thermal shock resistance with a higher amount of silicon nitride was observed means the composite SiC + Si<sub>3</sub>N<sub>4</sub> have better thermal shock resistance than the monolithic silicon carbide. Because hardness and fracture toughness for the SiC + Si<sub>3</sub>N<sub>4</sub> composites do not differ significantly from the values for SiC material, the reason for their better thermal shock resistance is unclear. One possible reason is slightly higher flexural strength values of composites than monolithic SiC materials (Table 2). The other possibility on the results is a difference in thermal properties of the materials. The higher thermal shock resistance of composites could be due to the better thermal shock behaviour<sup>37</sup> and lower thermal expansion coefficient of Si<sub>3</sub>N<sub>4</sub> than SiC.<sup>38</sup> The initiation crack length of annealed materials at 1850 °C was 20 μm shorter than to the hot pressed and heat treatment specimens at 1650 °C. Thermal shock tests, studied by indentation-quench method show enhanced resistance of the SiC + Si<sub>3</sub>N<sub>4</sub> compos-

ite and the monolithic SiC material with coarse microstructure, with higher indentation toughness. The explanation of this fact could be described by the  $R_{th}$  parameter<sup>21</sup>. This parameter reflects the fact that, to resist a given thermal shock, a material has to exhibit a high resistance to cracking, i.e. a high toughness, and has to have a low thermal stress. Therefore, it is important to design materials with specific microstructures to obtain an optimal state between resistance to initiation ( $R$ ) and resistance to propagation of crack ( $R'''$ ). Kalantar and Fantozzi<sup>2</sup> tested five silicon nitride materials with microstructures consisting of different aspect ratios. They showed that materials with elongated grains that are higher aspect ratio had higher  $\Delta T_c$ . The materials with elongated grains show several mechanisms of toughening, and so they may have stable crack propagation.

If the measured  $\Delta T_c$  values are compared with the calculated  $R$  parameter (Table 2), in most cases, the level of theoretic values is less than measured values and a linear relation exists between them.<sup>2</sup> In our case, the  $\Delta T_c$  values are lower for all tested specimens, but the largest difference is between theoretic  $R$  parameter and experimental estimated  $\Delta T_c$  of monolithic SiC and SiC + Si<sub>3</sub>N<sub>4</sub> composites annealed at 1850 °C. These materials have lower flexural strength (Table 2) values compared with fine-grained materials because the biggest and more strength degrading flaws were found.

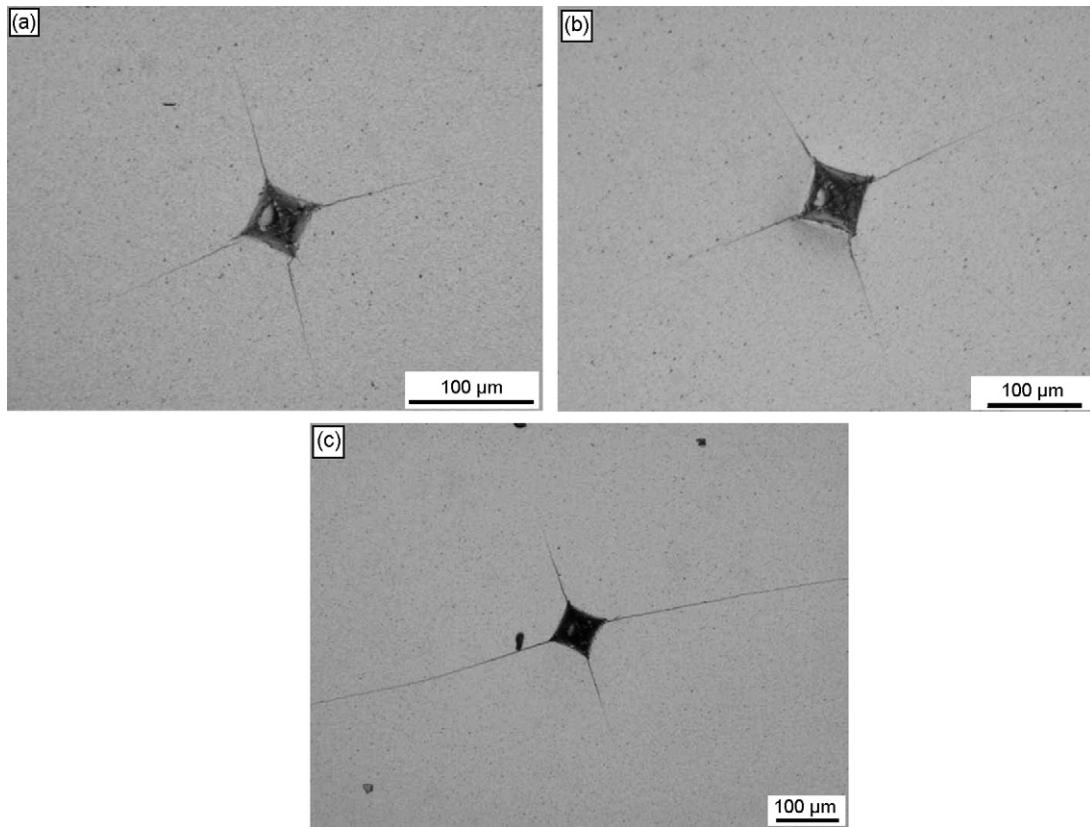


Fig. 4. Vickers indentation crack of SC-N10-1650: (a) before thermal shock; (b) after thermal shock ( $\Delta T=400^\circ\text{C}$ ); (c) after thermal shock ( $\Delta T=750^\circ\text{C}$ ).

For elimination of flexural strength values we compared our experimental results with data calculated with a theoretical model, which Tancret described elsewhere.<sup>39</sup> He proposed the  $R_m$  parameter, which can be measured without the knowledge of any material property ( $E$ ,  $K_c$ ,  $H$ ,  $\alpha$  and  $\nu$ ) or quenching medium characteristic ( $\Delta T$ ,  $h$ ). It is calculated directly from a measurement of radial crack lengths before and after thermal shock. The  $R_m$  parameter does not depend on the distribution of flaws in the material. The values  $\Delta T_c$  calculated according Tancret model are shown in Table 2. By comparing the results is clearly visible better agreement between our experimental values and Tancret model in fine-grained materials. In the case of plate-like structures are differences. Tancret model is valid for median-radial crack system. These types of cracks were observed mainly in fine microstructures. In the materials with higher aspect ratio of SiC grains we found mixed median-Palmquist system of cracks. This can be an explanation for disagreement of our results.

#### 4. Conclusion

Indentation tests have been used for the investigation of the toughness and thermal shock resistance behaviour of as-sintered and heat treated SiC materials and SiC + Si<sub>3</sub>N<sub>4</sub> composites.

The Si<sub>3</sub>N<sub>4</sub> addition has no influence on the indentation toughness but the heat-treatment especially at highest temperature of 1850 °C changed the microstructure significantly (the coarsening of the microstructure of experimental materials were

observed because  $\beta \rightarrow \alpha$  phase transformation of SiC take place) and leads to the indentation toughness increase.

This increase is connected with the present toughening mechanisms in the form of crack deflection, mechanical and frictional interlocking and crack branching.

It was found that both the silicon nitride addition and heat-treatment have a positive effect in the improvement of the thermal shock resistance of the investigated composites. However, more experiments are necessary to understand and explain the effect of silicon nitride that lead to improvements in thermal shock resistance.

#### Acknowledgements

This Work was partly supported by the National Slovak Grant Agency VEGA, project No. 2/7194/27, APVV-0171-06, LPP-0203-07, and NANOSMART, Centre of Excellence, SAS.

#### References

1. Falk, L. K. L., Microstructural development during liquid phase sintering of silicon carbide ceramics. *J. Eur. Ceram. Soc.*, 1997, **17**, 983–994.
2. Kalantar, M. and Fantozzi, G., Thermo-mechanical properties of ceramics: resistance to initiation and propagation of crack in high temperature. *Mater. Sci. Eng. A*, 2008, **472**, 237–280.
3. Hoffmann, M. J., Schneider, G. A. and Petzow, G., In *The Potential of Si<sub>3</sub>N<sub>4</sub> for Shock Applications—Thermal Shock and Thermal Fatigue Behaviour of Advanced Ceramics*, ed. G. A. Schneider and G. Petzow. Kluwer Academic, Boston, 1993, pp. 49–58.

4. Becher, F., Microstructural design of toughened ceramics. *J. Am. Ceram. Soc.*, 1991, **74**, 255–269.
5. Kim, Y.-W., Mitomo, M. and Hirotsuru, H., Microstructural development of silicon carbide containing large seed grains. *J. Am. Ceram. Soc.*, 1995, **80**, 99–105.
6. Padture, N. P., In situ-toughened silicon carbide. *J. Am. Ceram. Soc.*, 1994, **77**, 519–523.
7. Kim, J.-Y., Kim, Y.-W., Lee, J.-G. and Cho, K.-S., Effect of annealing on mechanical properties of self-reinforced alpha-silicon carbide. *J. Mater. Sci.*, 1999, **34**, 2325–2330.
8. Nader, M., Aldinger, F. and Hoffman, M. J., Influence of the  $\alpha/\beta$ -SiC phase transformation on microstructural development and mechanical properties of liquid phase sintered silicon carbide. *J. Mater. Sci.*, 1999, **34**, 1197–1204.
9. Cho, D. H., Kim, Y.-W. and Kim, W., Strength and fracture toughness of in situ-toughened silicon carbide. *J. Mater. Sci.*, 1997, **32**, 4777–4782.
10. Sciti, D., Guicciardi, S. and Bellosi, A., Effect of annealing treatments on microstructure and mechanical properties of liquid-phase-sintered silicon carbide. *J. Eur. Ceram. Soc.*, 2001, **21**, 621–632.
11. Kim, Y.-W., Mitomo, M., Emoto, H. and Lee, J.-G., Effect of initial  $\alpha$ -phase content on microstructure and mechanical properties of sintered silicon carbide. *J. Am. Ceram. Soc.*, 1998, **81**, 3136–3140.
12. Kim, Y.-W., Mitomo, M. and Hirotsuru, H., Grain growth and fracture toughness of fine-grained silicon carbide ceramics. *J. Am. Ceram. Soc.*, 1995, **78**, 3145–3148.
13. Cao, J. J., Moberly Chan, W. J., De Jonghe, L. C., Gilbert, C. J. and Ritchie, R. O., In situ toughened silicon carbide with Al-B-C additions. *J. Am. Ceram. Soc.*, 1996, **79**, 461–469.
14. Anstis, G. R., Chantikul, P., Lawn, B. R. and Marshall, D. B., A critical evaluation of indentation techniques for measuring fracture toughness. I. Direct crack measurements. *J. Am. Ceram. Soc.*, 1981, **64**, 533–538.
15. Evans, A. G. and Charles, E. A., Fracture toughness determinations by indentation. *J. Am. Ceram. Soc.*, 1976, **59**, 371–372.
16. Niihara, K., Morena, R. and Hasselman, D. P. H., Evaluation of  $K_{IC}$  of brittle solids by the indentation method with low crack-to-indent ratios. *J. Mater. Sci. Lett.*, 1982, **1**, 13–16.
17. Lankford, J., Indentation microfracture in the Palmqvist crack regime: implications for fracture toughness evaluation by the indentation method. *J. Mater. Sci. Lett.*, 1982, **1**, 493–495.
18. Shetty, D. K., Wright, I. G., Mincer, P. N. and Clauer, A. H., Indentation fracture of WC-Co cermets. *J. Mater. Sci.*, 1985, **20**, 1873–1882.
19. Laugier, M. T., New formula for indentation toughness in ceramics. *J. Mater. Sci. Lett.*, 1987, **6**, 355–356.
20. Quinn, G. D. and Bradt, R. C., On the Vickers indentation fracture toughness test. *J. Am. Ceram. Soc.*, 2007, **90**, 673–680.
21. Tancret, F., Comments on “Thermal shock resistance of yttria-stabilized zirconia with Palmqvist indentation crack” by G. Fargas, D. Cassellas, L. Llanes., M. Anglada. [*J. Eur. Ceram. Soc.* 23 (2003), 107–114]. *J. Eur. Ceram. Soc.*, 2006, **26**, 1517–1522.
22. Pettersson, P., Johnsson, P. and Shen, Z., Parameters for measuring the thermal shock of ceramic materials with an indentation-quench method. *J. Eur. Ceram. Soc.*, 2002, **22**, 1883–1889.
23. Andersson, T. and Rowcliffe, D. J., Indentation thermal shock test for ceramics. *J. Am. Ceram. Soc.*, 1996, **79**, 1509–1514.
24. Hasselman, D. P. H., United theory of thermal shock fracture initiation and crack propagation in brittle ceramics. *J. Am. Ceram. Soc.*, 1969, **52**, 600–604.
25. Collin, M. and Rowcliffe, D., Analysis and prediction of thermal shock in brittle materials. *Acta Mater.*, 2000, **48**, 1655–1665.
26. Hasselman, D. P. H., Thermal stress resistance parameters for brittle refractory ceramics: a compendium. *Am. Ceram. Soc. Bull.*, 1970, **49**, 1033–1037.
27. Takeda, Y. and Maeda, K., Thermal shock resistance of high thermal conductive SiC ceramics. *J. Ceram. Soc., Jpn. Int.*, 1991, **99**, 1113–1116.
28. Wang, H. and Singh, R. N., Thermal shock behavior of ceramics and ceramic composites. *Int. Mater. Rev.*, 1994, **39**, 228–244.
29. Maensiri, S. and Roberts, S. G., Thermal shock resistance of sintered alumina/silicon carbide nanocomposites evaluated by indentation techniques. *J. Am. Ceram. Soc.*, 2002, **85**, 1971–1978.
30. Hvizdoš, P., Jonsson, D., Anglada, M., Anné, G. and Van Der Biest, O., Mechanical properties and thermal shock behaviour of an alumina/zirconia functionally graded material prepared by electrophoretic deposition. *J. Eur. Ceram. Soc.*, 2007, **27**, 1365–1371.
31. Rui-Xia, S., Yan-Sheng, Y., Jia, L. and Dong-Zhi, W., Influence of cobalt phase on thermal shock resistance of  $Al_2O_3$ -TiC composites evaluated by indentation technique. *Mater. Res. Bull.*, 2008., doi:10.1016/j.mater.resbull.2007.11.001.
32. Yang, Z.-H., Jia, D.-Ch., Zhou, Y., Meng, Q.-Ch., Shi, P.-Y. and Song, Ch.-B., Thermal shock resistance of in situ formed SiC-BN composites. *Mater. Chem. Phys.*, 2008, **107**, 476–479.
33. Ding, S., Zeng, Y.-P. and Jiang, D., Thermal shock resistance of in situ reaction bonded porous silicon carbide ceramics. *Mater. Sci. Eng. A*, 2006, **425**, 326–329.
34. Rice, R. W., Wu, C. C. and Borchelt, F., Hardness—grain-size relations in ceramics. *J. Am. Ceram. Soc.*, 1994, **77**, 2539–2553.
35. Do-Hyeong, K. and Hee Chong, K., Toughening behavior of silicon carbide with additions of yttria and alumina. *J. Am. Ceram. Soc.*, 1990, **73**, 1431–1434.
36. Lee, S. K., Moretti, J. D., Readey, M. J. and Lawn, B. R., Thermal shock resistance of silicon nitride using an indentation-quench test. *J. Am. Ceram. Soc.*, 2002, **85**, 279–281.
37. Schneider, G. A., Thermal shock criteria for ceramics. *Ceram. Int.*, 1991, **17**, 325–333.
38. Munz, D. and Fett, T., In *Ceramics. Mechanical Properties, Failure Behaviour, Materials Selection, Springer Series in Materials Science*, ed. R. Hull, R. M. Osgood, H. Sakaki and A. Zunger. Springer-Verlag, Berlin-Heidelberg-New York, 1999, p. 229.
39. Tancret, F. and Osterstock, F., The Vickers indentation technique used to evaluate thermal shock resistance of brittle materials. *Scripta Mater.*, 1997, **37**, 443–447.